

---

CHAPTER III

---

---

OBSERVATIONS

---

### A) General Observations :

The mollasses is produced as the by product of sugar industry and it is utilized for the production of alcohol in distillery. The alcohol is obtained by fermenting the diluted mollasses with yeast. The waste material in the form of a liquid is produced during the process and it is released out in the form of distillery effluent or spent wash. This causes tremendous depletion in the oxygen content of the water where it is discharged.

During the present investigations, to study the physico-chemical properties of the spent wash used in aquaria the following parameters were studied : namely temperature, pH, hardness and dissolved oxygen. The results obtained are recorded in Table No.2 and shown in fig. 1, 2 and 3.

Fluctuations in the values of the parameters are evident from the table and figures. The temperature varied from  $27^{\circ}\text{C}$  to  $32^{\circ}\text{C}$  during day. The mean temperature being  $29.5^{\circ}\text{C}$ . The pH of tap water used for acclimatization of fish was 7.5 which gradually decreased after addition of distillery effluent in it for making the concentrations of strength 1%, 2%, 3%, 4% and 5%. The corresponding pH values were observed to be 5.5, 5.0, 4.5, 4.1 and 4.0 respectively. The  $\text{CaCO}_3$  hardness of tapwater was 53.82 mg/l. This increased gradually after the addition of distillery effluent in it. The values of hardness were 107.63, 199.64, 255.20, 320.32 and 378.48 mg  $\text{CaCO}_3$ /l. for 1%, 2%, 3%, 4% and 5% concentrations respectively. The DO values gradually

Ob. No.	Conc. of distillery effluent	Mean temp.	pH	Hardness CaCO <sub>3</sub> mg/l	DO mg/l.
1.	Tap water	27.5°C	7.5	53.82	5.0
2.	1% dist. effluent	27.5°C	5.5	107.63	4.2
3.	2% dist. effluent	27.5°C	5.0	199.64	4.0
4.	3% dist. effluent	27.5°C	4.5	255.20	3.8
5.	4% dist. effluent	27.5°C	4.1	320.32	3.5
6.	5% dist. effluent	27.5°C	4.0	378.48	3.3

Table No.2 : Showing the values of Physico-chemical parameters of tap water and the same at different concentrations of distillery effluent.

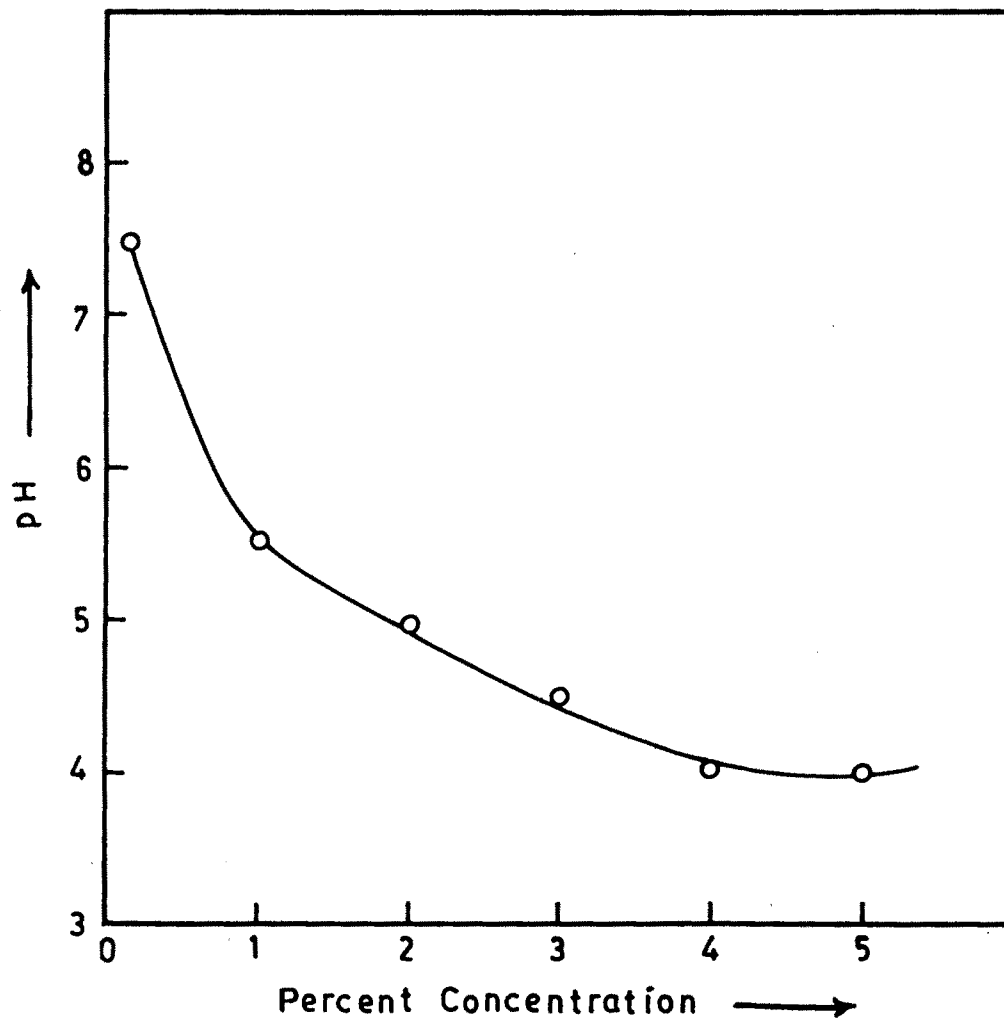


Fig. 1 — SHOWING pH VALUES AT DIFFERENT CONCENTRATIONS OF DISTILLERY EFFLUENT.

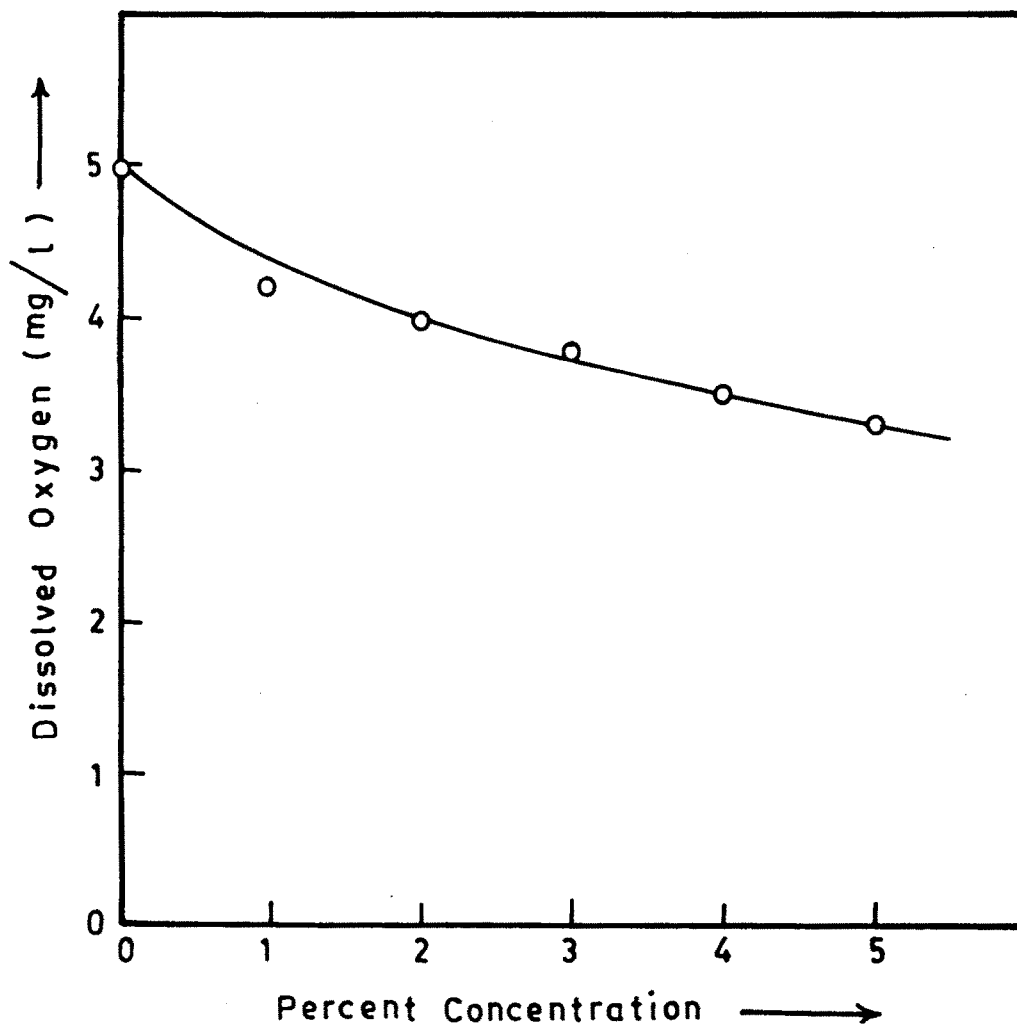


Fig. 2 — SHOWING DISSOLVED OXYGEN VALUES  
IN mg/l AT DIFFERENT CONCENTRATIONS  
OF DISTILLERY EFFLUENT .

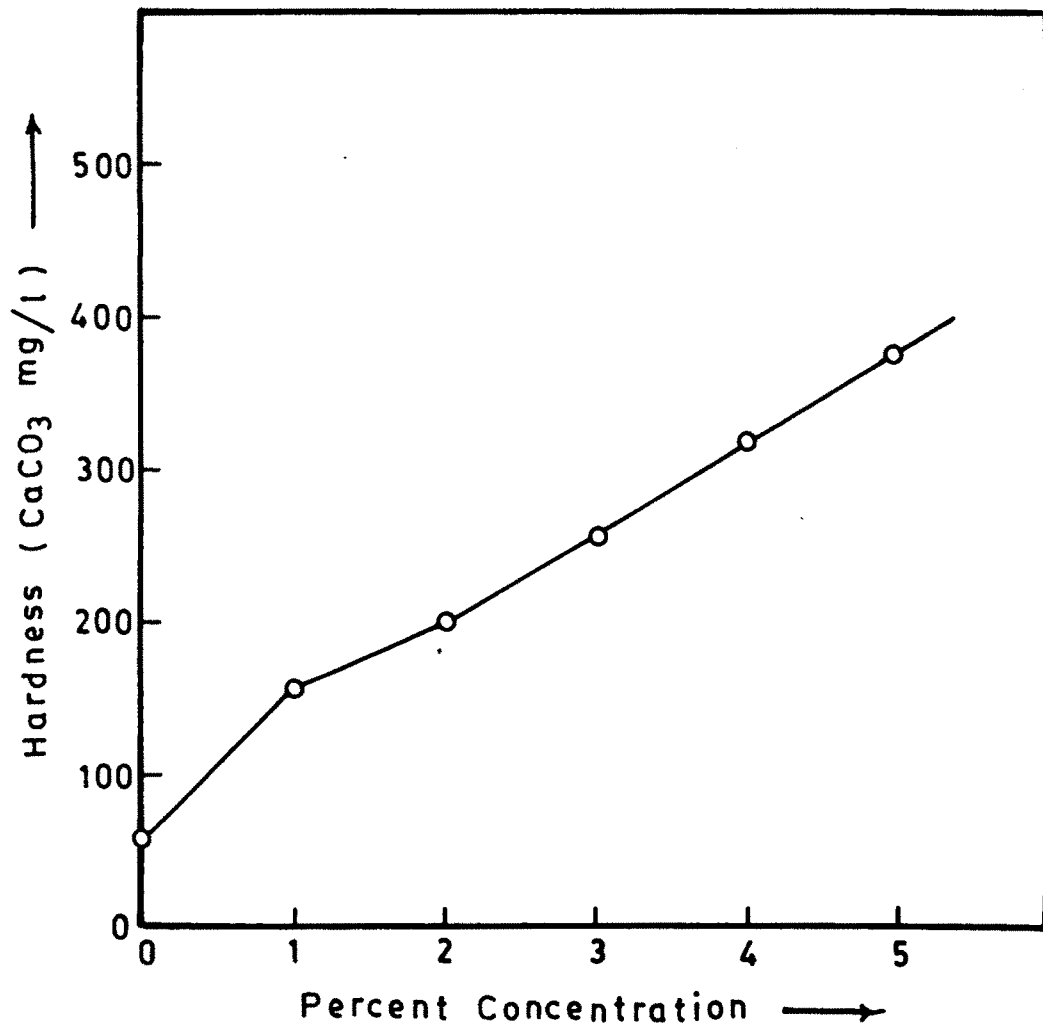


Fig. 3 — SHOWING VALUES OF CaCO<sub>3</sub> HARDNESS IN mg/lit AT DIFFERENT CONCENTRATIONS OF DISTILLERY EFFLUENT .

decreased from 5 mg/l to 3.3 mg/l for the higher concentrations.

B) Determination of LC 50 values :

Determination of LC 50 values for I.mossambica and R.daniconius was carried out using different concentrations of distillery effluent. The results of the rate of mortality are shown in Table No.3 and 4 and are shown in fig. 4. They show that 50% mortality of I.mossambica occurred at 2.5% concentration and hence, the LC 50 value for it is 2.5%. In R.daniconius 50% mortality was achieved at 3.1% conc. and therefore the LC 50 value for it is estimated to be 3.1%.

C) Fish Behaviour :

Following behavioural pattern was observed in both types of acclimatized fishes in the order given below, when they were transferred to experimental aquaria having different concentrations of distillery effluent.

- (i) Fishes were excited in the beginning for some time and then they became steady, with erratic and occasional jerky movements.
- (ii) There was a gradual decrease in opercular movement of the fish.
- (iii) This was followed by the slow movement of the fish towards the surface of water assuming a diagonal position.
- (iv) The fish became inverted (belly upwards) and floated near the surface for some time before finally settling down at the bottom of aquarium.

% Concs.	No. of fishes used	No. of dead fishes					% mortality at 48 hrs
		12 hrs.	24 hrs.	48 hrs.	72 hrs.	96 hrs.	
1 %	10	Nil	Nil	2	4	4	20 %
2 %	10	Nil	2	2	4	2	40 %
3 %	10	1	2	3	4	-	60 %
4 %	10	2	3	2	2	-	70 %
5 %	10	10	-	-	-	-	100 %
Control (Normal)	10	Nil	Nil	Nil	Nil	Nil	0.0 %

Table No. 3 : Showing Mortality Record <sup>of</sup> I. mossambica  
at different concentrations of distillery-  
effluent.

% Concs.	No. of fishes used	No. of dead fishes					% mortality at 48 hrs.
		12 hrs.	24 hrs.	48 hrs.	72 hrs.	96 hrs.	
1 %	10	Nil	Nil	Nil	Nil	Nil	0.0 %
2 %	10	Nil	Nil	2	4	4	20 %
3 %	10	Nil	Nil	5	5	-	50 %
4 %	10	Nil	3	4	3	-	70 %
5%	10	10	-	-	-	-	100 %
Control (Normal)	10	Nil	Nil	Nil	Nil	Nil	0.0%

Table No. 4 : Showing Mortality Record <sup>of</sup> R. daniconius  
at different concentration of distillery -  
effluent.

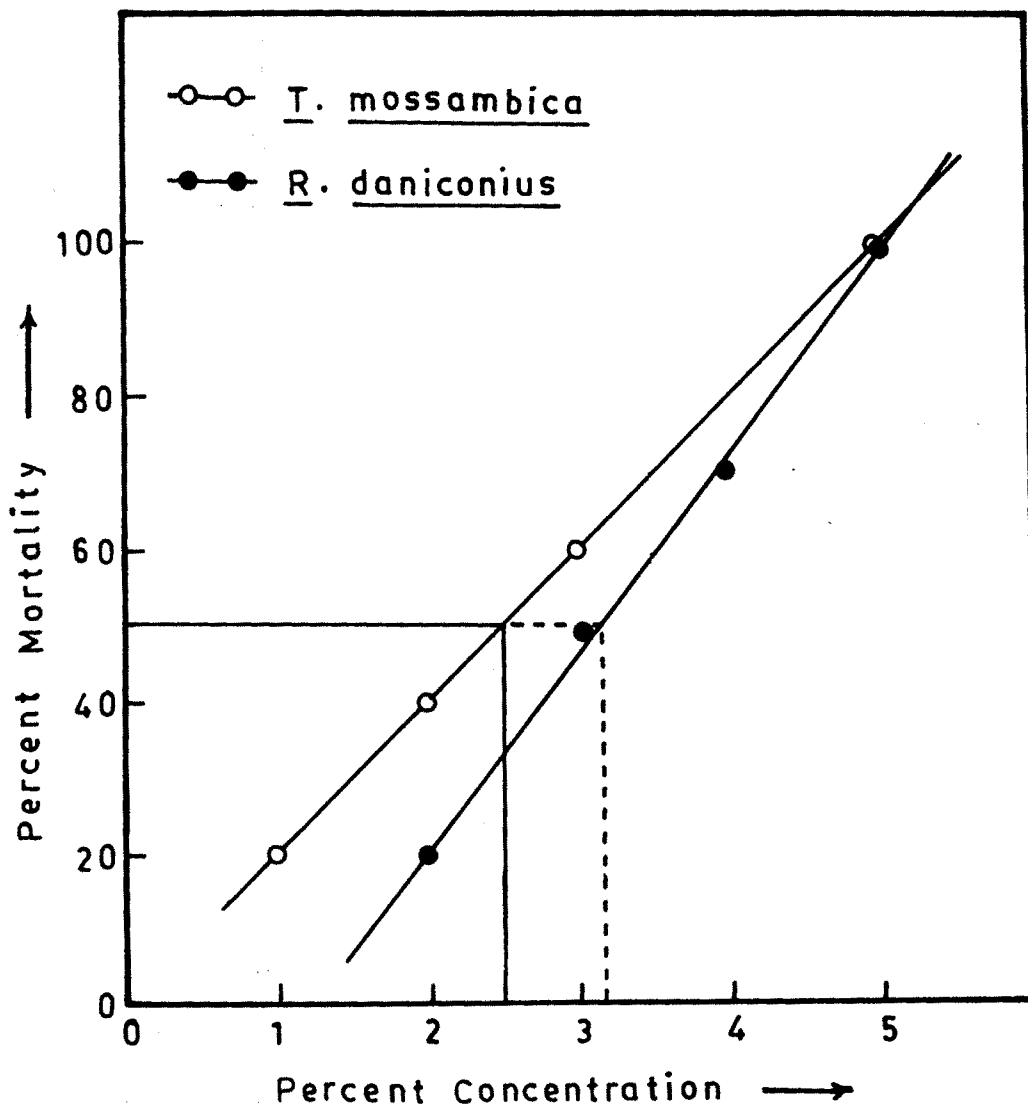


Fig. 4 — SHOWING LC 50 VALUES FOR T. mossambica AND R. daniconius AT DIFFERENT CONCENTRATIONS OF DISTILLERY EFFLUENT .

- (v) The fish appeared to be completely suffocated and did not show any response to touch.
- (vi) The mortality was evident because of the absence of any motion or respiration since there was no movement of operculum.
- (vii) At times mouth and operculum remained opened at the end.
- (viii) There was abundant discharge of mucus on the gill and skin.

It appears that suffocation (asphyxiation) of the fish was the ultimate result due to strained respiration when it was exposed to lethal concentration of the distillery effluent.

#### D) Histology and Histopathology :

##### (i) GILL :

##### Tilapia mossambica :

The microanatomical structure of gill of the control fish and the histopathological changes occurring due to different concentrations of distillery effluent are shown in Plate No. 1 (Figs. 1-12).

##### Histology :

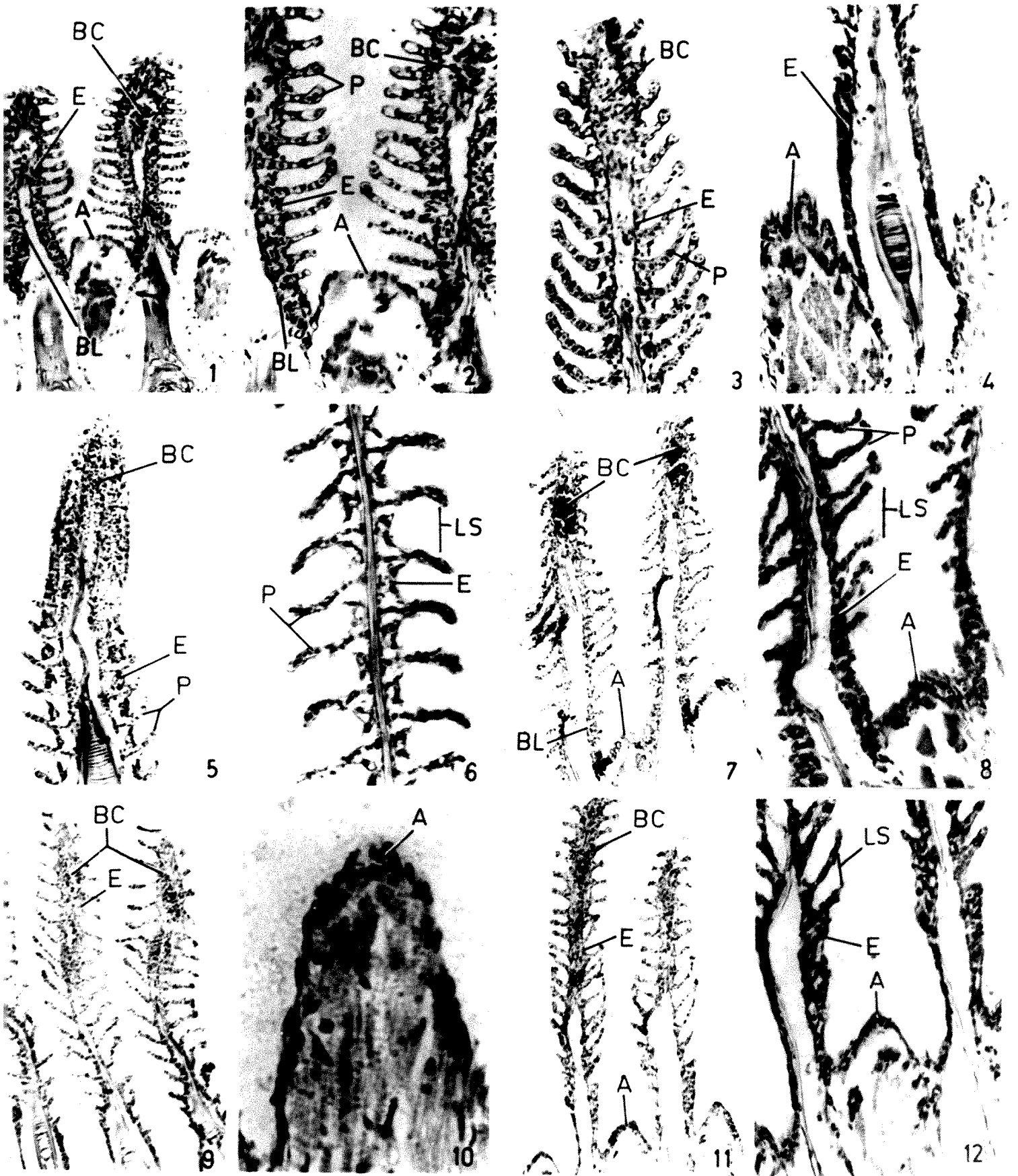
The histological structure of gill of I. mossambica showed similarities to many fresh water teleosts. There are four pairs of gills and two rows of primary gill lamellae borne on the ceratobranchial and epibranchial segments of each gill arch. Each gill is supported by a bony element. From the primary gill filaments several regular semilunar projections arise on the dorsal and ventral sides. They are secondary gill lamellae. They are separated by interbranchial septum, so that

### CAPTIONS TO FIGURES

Plate No.1 : Histopathological changes in the gill of  
I. mossambica stained with H-E.

- Fig.1 T.S. of normal gill showing primary, secondary gill lamellae and interlamellar region, Epithelium (E), Blood cells (BC) and Acidophil cells (A). X 100. *Basal lamella (BL)*
- Fig.2 A magnified view of T.S. of normal gill showing Epithelium (E), Pillar cells (P), Blood cells (BC), Acidophil cells (A) and Basal lamella (BL). X 200.
- Fig.3 T.S. of gill exposed to 1% conc. showing thickening of general epithelium (E), Pillar cells (P) are slightly bulged. Bulging of distal end of primary lamellae with blood cells (BC). X 200.
- Fig.4 T.S. of gill exposed to 1% conc. showing thickening of epithelium (E) and increased Acidophil cells (A). X 200.
- Fig.5 T.S. of gill exposed to 2% conc. showing curling of secondary lamellae, thinning of pillar cells (P), and thickening of epithelium (E). X 100. *Blood cells (BC)*
- Fig.6 T.S. of gill exposed to 2% conc. showing thinning of pillar cells (P), thickening of epithelium (E) and increased interlamellar space (LS). X 450.
- Fig.7 T.S. of gill exposed to 3% conc. showing curling of secondary lamellae. Accumulation of blood cells at distal end of primary lamellae (BS) and increased acidophil cells (A). X 100. *Blood cells (BC), Basal lamella (BL)*
- Fig.8 T.S. of gill exposed to 3% conc. showing curling of secondary lamellae, degeneration of epithelium (E), swollen pillar cells (P), increased interlamellar space (LS) and acidophils (A). X 200.
- Fig.9 T.S. of gill exposed to 4% conc. showing degeneration of epithelium (E) and decreased blood cells at the distal end (BC). X 100.
- Fig.10 T.S. of gill exposed to 4% conc. showing a magnified view of interlamellar region with increased acidophil cells (A). X 450.
- Fig.11 T.S. of gill exposed to 5% conc. showing increased degeneration of epithelium (E), increased blood cells (BC) and acidophils (A). X 100.
- Fig.12 T.S. of gill exposed to 5% conc. showing progressive degeneration of epithelium (E), marked changes in interlamellar space (LS) and accumulation of acidophils (A). X 200.

# PLATE NO. 1



the lamellae of two rows are free at their distal ends.

Microscopic structure of the primary gill consists of a vascular layer (fig. 1 & 2) in the middle with an envelope of epithelial cells and thin layer of connective tissue in between. The pillar cells provide the support to secondary lamellae. They are arranged one after the other, between adjacent capillaries of the secondary lamellae (fig. 1 & 2). The secondary lamellae are supported by cartilagenous structures.

The epithelial layer shows presence of numerous mucous gland cells, which are distributed over the epithelial covering of the gill arch, the bases of secondary lamellae and the general surface of primary gill filament. The acidophil cells (fig. 1 & 2) are seen at the bases of primary and secondary lamellae. The central lamellar portion of the primary gill shows many blood cells (fig. 1 & 2).

#### Histopathology :

Accumulation of mucus was often seen with naked eye on the skin and opercula of overturned fishes before fixation. But microscopically the mucous covering of gill surface appeared normal. No damage of secondary lamellae was observed. The epithelium was intact at lamellar margin. Interlamellar space was uniform as in the control.

#### 1% Conc. :

The general epithelial covering of gill filament appeared largely unaffected. Slight enlargement of the marginal channel

and filamental sinus was observed (fig.3,4). A slight thickening in the epithelium of the secondary lamellae occurred. The pillar cells were also slightly bulged. These changes resulted in curling of the secondary lamellae. The lamellar blood spaces were also slightly enlarged (fig.3). There was no increase in acidophil cells and mucous cells.

2% Conc. :

Here the changes were more pronounced than in the earlier case. Accumulation of mucous at the gill opercula and over the general gill surface was significant. An uneven curling occurred in the secondary lamellae. Some of them showed thinning and shortening characters. The apical secondary gill lamellae were more affected than the basal ones (fig.5,6).

There was an increase in the interlamellar space. Thinning of the pillar cells was evident(Figs.5,6). Primary gill arch was reduced in its thickness. The epithelium of the primary filament showed a slight detachment from the basement membrane (fig.5,6). The blood space at the distal end of primary gill filament was unaffected. However, it was reduced in the secondary lamellae. The initiation of histolysis was evident at the tip of primary gill filament (fig.5 & 6). ✓ There was an increase in the number of acidophil and mucous cells.

3% conc. :

The histopathological results at 3% distillery effluent exposure showed much drastic changes in gill rachis, secondary gill lamellae, acidophil cells and blood spaces.

The gill epithelium of primary and secondary gill lamellæ was covered by a thin layer of mucous film. However it was lost during the processing of the tissues for histological preparations. The supporting rod of the primary gill became very thin. The secondary lamellæ were reduced in their thickness. They showed an uneven curling nature. It was pronounced in comparison with the earlier observations (fig. 7 & 8). The secondary lamellæ showed degenerative changes at their bases. The epithelium was found to be shifted considerably from the basement membrane. The blood space at the distal portion of primary gill filament showed swelling and accumulation of blood cells. Swelling of the pillar cells was also seen (fig. 7 and 8). The acidophil cells increased in their number (fig. 7 and 8).

4% Conc. :

The excessive mucous secretion and its accumulation on the surface epithelium was evident (fig. 9,10) at this concentration. The primary lamellæ showed progressive degenerative changes in the central supporting rod (fig. 9,10). Enhanced accumulation of the blood cells occurred in blood spaces. They were also found to be scattered in the degenerated regions of subepithelial space of the primary lamellæ (fig. 9,10). Scattering of blood cells was also observed in the gill rachis, indicating the rupture of lamellar capillaries. Major degenerative changes were also evident in the secondary lamellæ. Thinning of the epithelial and pillar cells was more prominent at this concentration (fig. 9,10). Their number appeared to be reduced. Nearly 50% secondary lamellæ showed shortening due to

the loss of cells. It indicated the enhancement of histolysis and beginning of sloughing. The curling of the secondary lamellae was further enhanced (fig.9,10).

The lamellae at the basal region of the primary gill showed pronounced sloughing. The acidophil cells were prominent in the interlamellar region (fig.9,10).

5% Conc. :

The microscopic examination of the gill at 5% of distillery effluent exposure revealed more thinning of secondary gill lamellae, especially in the general epithelial cells and pillar cells. The detachment of the epithelial surface in the primary gill lamellae was evident in this experiment also. A progressive degeneration occurred in the supporting structure of the primary gill lamellae (fig.11,12). Accumulation of the blood cells in the intercellular space occurred due to degeneration of septum and it was more pronounced. Most of the blood cells showed swelling and haemolysis (fig.11,12) and hence groups of blood cells with spindle shaped nuclei could be seen. This process led to the formation of haematomas (fig.11,12). Similar changes were observed surrounding the surface of the gill rachis.

Acute changes were seen in the secondary lamellae at this concentration. Almost all of them showed shortening due to loss of pillar cells (fig.11,12); leaving very small gaps in the intercellular region. These gaps were filled with blood cells (fig.11,12). In certain regions of the secondary lamellae, formation of the haematomas occurred. The secondary lamellae

tended to overlap one another in the middle region. At the basal region of the primary lamellae, almost all secondary lamellae were found to be entangled in the mucus material. Their epithelium was found to be merged with the epithelia of the primary lamellae (fig.11,12). These alterations clearly indicated the degenerative changes in the gill structure of the fish. The acidophil cells were found to be accumulated in the interlamellar region (fig.11,12).

#### Rasbora daniconius :

The histological structure of normal gill and histopathological alterations occurring therein due to the distillery effluent exposure are shown in Plate No.2 (fig.1-12).

#### Histology :

The anatomical and histological structures of gill of R.daniconius are more or less identical to that of I.mossambica and other freshwater teleosts. It shows the usual structures such as primary gill lamellae, secondary gill lamellae, multi-layered epithelial covering on the lamellae; containing mucous cells, acidophil cells and pillar cells in secondary lamellae (fig.1,2). There are no differences in the distribution of blood vessels and blood spaces. However, the secondary gill lamellae of R.daniconius differ from those of I.mossambica in their length. They are longer in R.daniconius (fig.1,2).

#### Histopathology :

Pathological changes in the gills of R.daniconius exposed

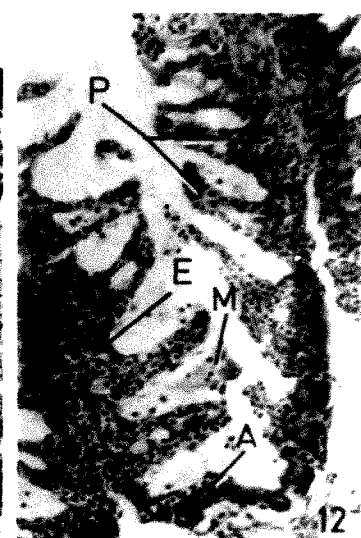
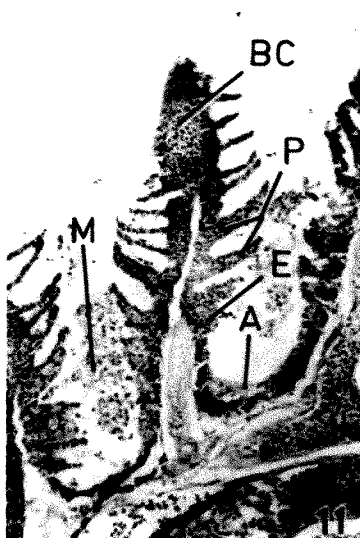
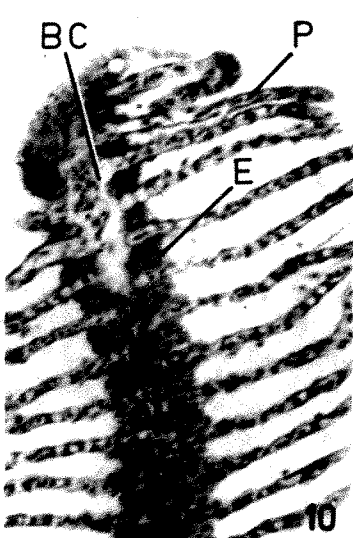
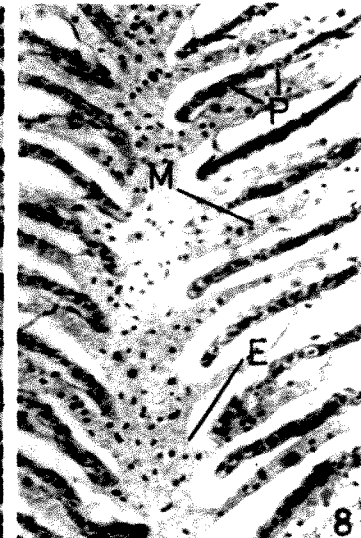
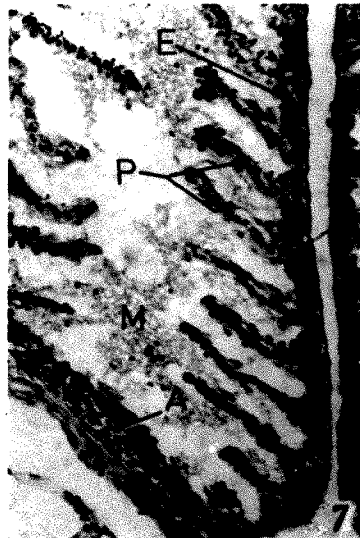
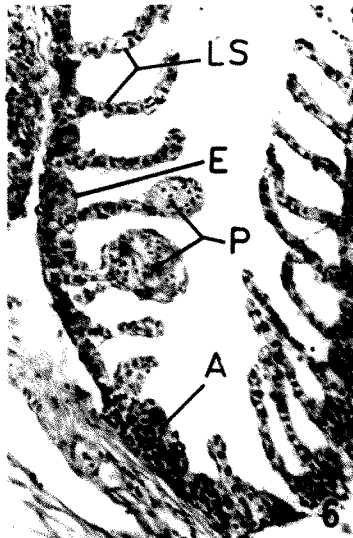
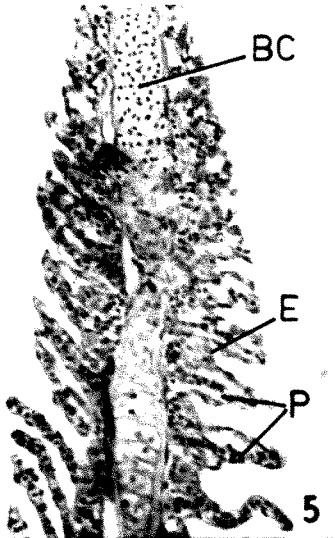
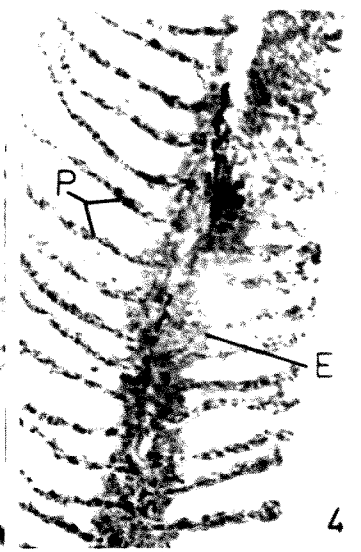
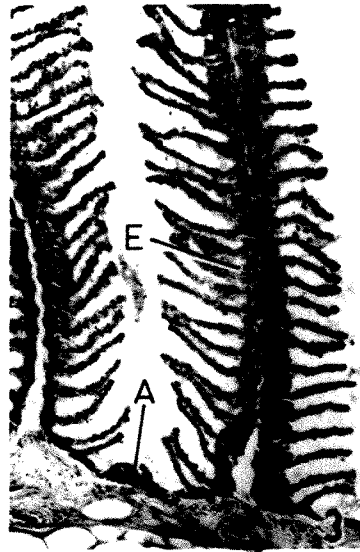
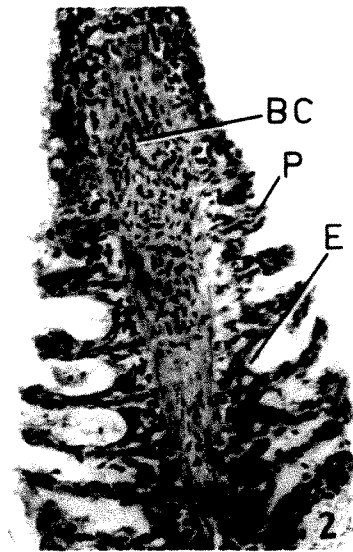
## CAPTIONS TO FIGURES

Plate No.2 : Histopathological changes in the gill of  
R. daniconius stained with H-E.

- Fig.1 T.S. of normal gill showing primary, secondary gill lamellae, epithelium (E) and blood cells (BC). X 60.
- Fig.2 A magnified view of T.S. of normal gill showing epithelium(E), pillar cells (P) and blood cells (BC). X 200.
- Fig.3 T.S. of gill exposed to 1% conc. showing thickening of epithelium (E) and accumulation of acidophils (A). X 100.
- Fig.4 A magnified view of T.S. of gill exposed to 1% conc. showing swollen pillar cells (P) and thickened epithelium (E). X 200.
- Fig.5 T.S. of gill exposed to 2% conc. showing a marked swelling of epithelium (E) and pillar cells (P) with accumulation of blood cells at the distal end (BC). X 200.
- Fig.6 T.S. of gill exposed to 2% conc. showing peculiar thickening of pillar cells (P) at distal end, thickening of epithelium (E), increased interlamellar space (LS) and accumulation of acidophils (A). X 200.
- Fig.7 T.S. of gill exposed to 3% conc. showing increased mucus between two gill filaments (M), thickened epithelium (E), pillar cells (P) and accumulation of acidophils (A).: X 200.
- Fig.8 T.S. of gill exposed to 3% conc. showing increased mucus (M), between secondary lamellae thickened epithelium (E) and pillar cells (P). X 450.
- Fig.9 T.S. of gill exposed to 4% conc. showing degeneration of epithelium (E), Swollen pillar cells (P) and accumulation of acidophils (A). X 200.
- Fig.10 T.S. of gill exposed to 4% conc., a magnified view of distal end showing degenerated epithelium (E), pillar cells (P) and accumulation of blood cells (BC). X 200.
- Fig.11 T.S. of gill exposed to 5% conc. showing mucus (M) in between two lamellae, increased degeneration of epithelium (E), fused pillar cells (P). Accumulation of acidophils (A) and blood cells (BC). X 100.
- Fig.12 A magnified view of T.S. of gill exposed to 5% conc. showing progressive degeneration of epithelium (E), increased mucus secretion (M) and fused pillar cells (P). X 200.

*Acidophils (A)*

# PLATE NO. 2



to the different concentrations of distillery effluent are shown in the Plate No.2 (fig.3 to 12). The changes occurred in this fish are slightly different than those observed in I.mossambica.

The first sign of the toxic effect of the distillery effluent was evidenced by the covering of a thin mucus secretion over the opercula and the skin. The mucus also accumulated between the primary gill lamellae.

1% Conc. :

The primary lamellae showed no change at the basal region. The degenerative changes, however, were evident in their apical portion (fig.4). The space at the apical end was filled with blood cells. There was no evidence of damage to the capillary at this concentration. The supporting rod showed no alterations.

The epithelium of secondary lamellae showed swelling (fig.3,4). It was evident in epithelial, mucus and pillar cells. This led to the formation of vacuoles in these cellular elements (fig.3,4). The lamellae at the base of primary lamellae showed curling and they met at the tips. The mucus cells of secondary lamellae became swollen. At the distal end few secondary lamellae were found to be fused and showed degenerative changes (fig.3,4) which left a cellular debris. No accumulation of additional blood cells was evidenced in the secondary gill lamellae.

2% Conc. :

Massive secretion of mucus occurred on the gill surface and because of it, there was an entangling of the secondary lamellae, particularly at their distal ends. The epithelial lining of

primary gill lamellae showed swelling (fig.5,6). No detachment of this layer from the basement membrane occurred at this concentration. There was no evidence of capillary damage in the primary lamellae. The epithelial wall of secondary lamellae was acutely inflamed (fig.5,6). Few of the secondary lamellae showed the formation of gill lesions (fig.6). Pillar cells were also enlarged (fig.5,6) and they left large gaps between them. Secondary lamellae at distal end appeared to be fused and merged with each other. Hence, in this region the details of the histology are not discernible. About 30 to 40 percent of the secondary lamellae showed curling. Some of them showed thinning and degenerative changes. Acidophil cells were moderate in size and number (fig.5,6).

3% Conc. :

Acute changes in the histomorphological structure of gill lamellae were observed at this concentration. Massive mucus secretion occurred on operculum and gill surface. Thickened and coagulated mucus coating on the gill epithelia was clearly seen. Further thickening and swelling of the epithelial lining of primary gill lamellae was more pronounced than in the earlier experiment. Hypertrophied mucous cells at the base were prominent, whereas at the apical region they were destroyed (fig.7,8). In the interlamellar space there occurred a mixture of mucous and blood cells (fig.7,8). At certain places the blood was found to be diffused in the secondary lamellae, thus indicating capillary damage and haemorrhage. Further uneven curling occurred at this

concentration. The space between two gill lamellae was totally packed with mucus secretion (fig.7,8). The enlargement of mucus, pillar and epithelial cells was prominent and it led to the detachment of epithelial layer from the basement membrane (fig.7,8). This process formed subepithelial space. This space was filled with blood cells due to the haemorrhagic condition. Haematomas were observed in the secondary lamellae at the basal region and also at the tip of primary gill lamellae (fig.7,8). Acidophil cells enlarged prominently in their size and number.

4% Conc. :

An increased thickening of the primary gill lamellar epithelium was found at this concentration. The epithelial cells and mucous cells were swollen and hypertrophied further (fig.9, 10). The apical region of the gill lamellae was distorted. The space in it was filled with blood cells. Very few of them remained intact and others were destroyed (fig.9,10). The central space of the primary gill was filled with deformed blood cells indicating haemorrhagic condition.

More acute and pronounced changes occurred in the secondary gill lamellae. They showed intense curling towards apical portion of the primary gill lamellae (fig.9). Further thinning and elongation of the gill filament was seen in a few secondary lamellae. In others their basal portions were found to be swollen and hypertrophied. In this region the pillar and mucous cells were enlarged tremendously. The distal secondary lamellae appeared to be fused at the tips and they were merged with each

other (fig.9,10). Mucous cells in this region were completely destroyed. The intercellular spaces of secondary lamellae were filled with blood (fig.9,10).

5% Conc. :

Low magnification revealed an overall picture of the acute changes occurred at this concentration. The epithelial linings of the secondary lamellae at the tips were thickened considerably (fig.11,12). Several secondary lamellae appeared to be fused together (fig.12) and in parts destroyed? Their appearance was similar to that in I.mossambica. In some, the distal parts of filaments were missing due to sloughing. The few mucous cells still present, showed massive secretion which covered the entire gill surface. The haemorrhage or inflamed areas were present and they were filled with the blood cells. The mucous cells at the tip of primary gill lamellae were absent. The lifting of epithelium from basement membrane created a large subepithelial space. This space was filled with blood due to which accumulated the bursting of capillaries. The sloughing of epithelial cells was more pronounced and it was indicated by the occurrence of detached cellular debris in the mucus present between two primary gill lamellae (fig.12). The region that surrounds the cartilagenous gill rachis also showed haemorrhagic condition (fig.11).

(ii) LIVER :

I.mossambica :

The structure of the liver of normal and treated I.mossambica with different concentrations of distillery effluent are

shown in Plate No.3 (fig.1 to 12).

#### Histology :

The liver of I.mossambica has two lobes. The gall bladder is embedded in the left lobe. Each lobe is composed of lobules. In turn they are composed of tubular glands. In them the blood bathes the tiers of cells on one side while the bile is secreted into the canal on the other side.

The liver is composed of polyhydral hepatic cells. Each hepatic cell contains a granular cytoplasm and central nucleus. They are arranged in a cord like formation (fig.1,2). A large number of blood sinusoids occur in the hepatic mass of these cords. The wall separating the neighbouring cords are found to be two cells thick. Thin bile canaliculi are seen between the hepatic cells. The bile duct is very prominent in between the hepatic lobules. At some places, central veins are clearly visible (fig.1,2). The pancreatic tissue containing Islet-cells are easily recognizable. They are bigger in size and have markedly different staining properties.

#### Histopathology :

The histopathological alterations occurring in the liver of I.mossambica exposed to various concentrations of the distillery effluent are shown in Plate No.3 (figs. 3 to 12).

#### 1% Conc.

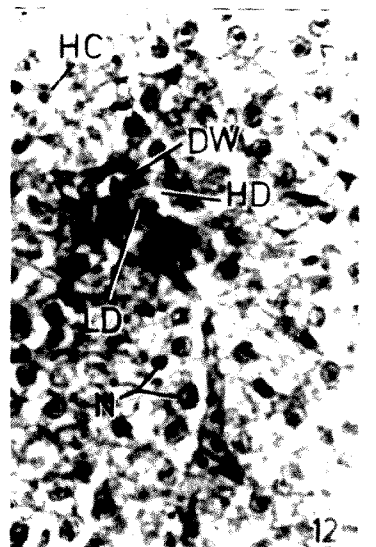
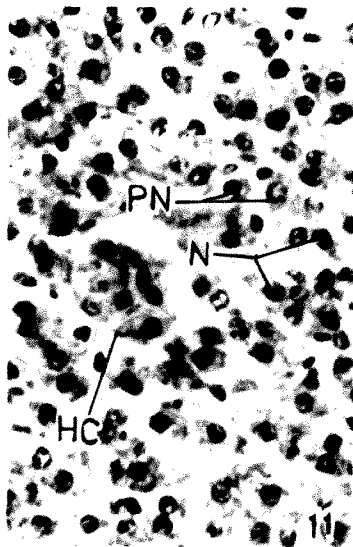
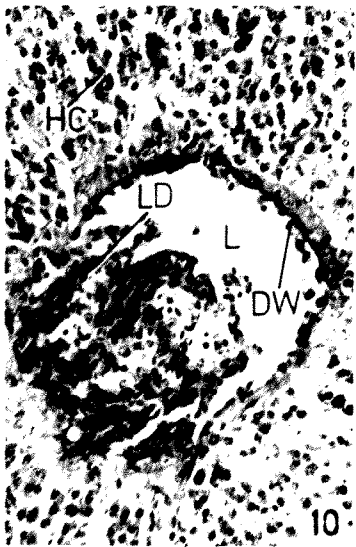
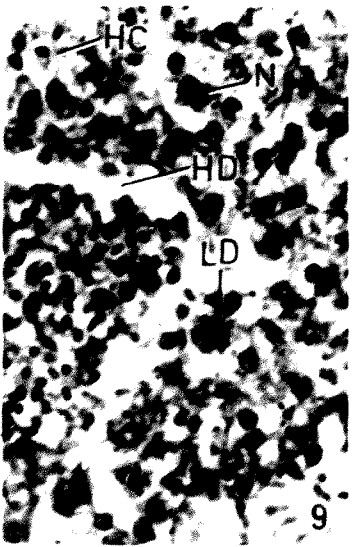
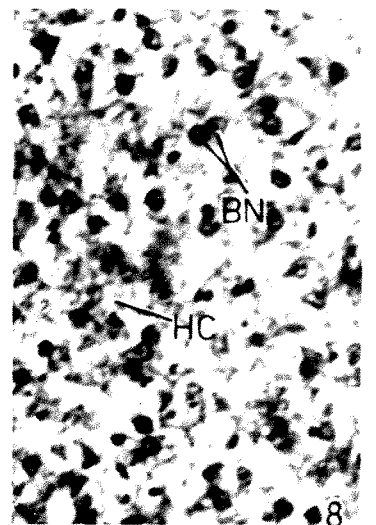
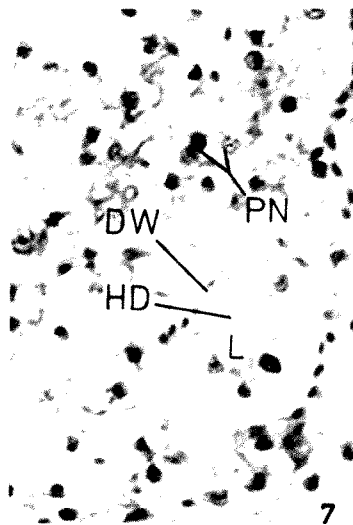
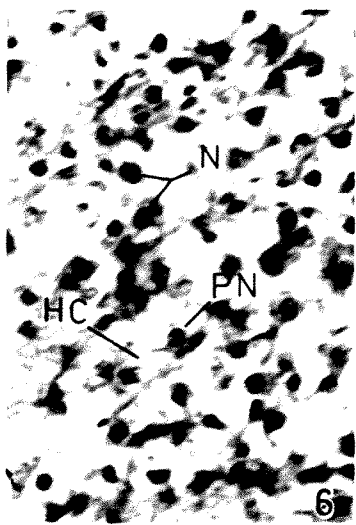
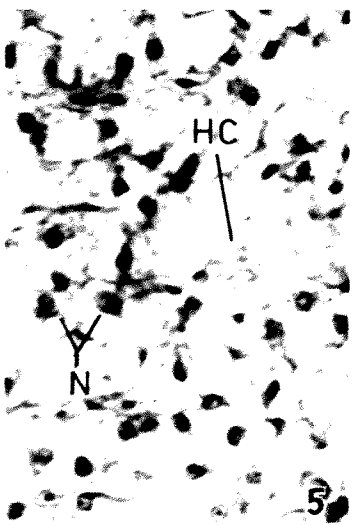
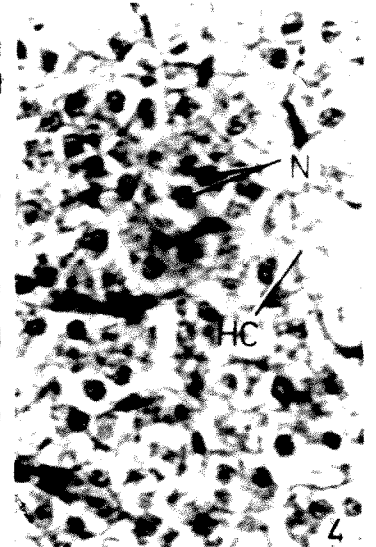
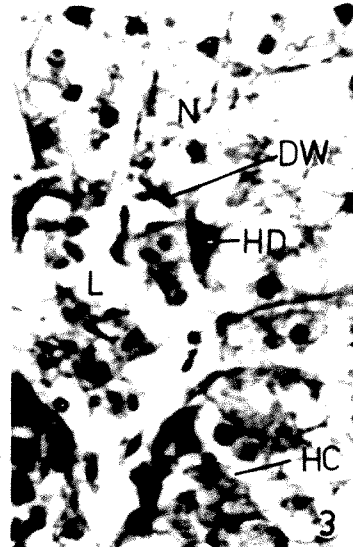
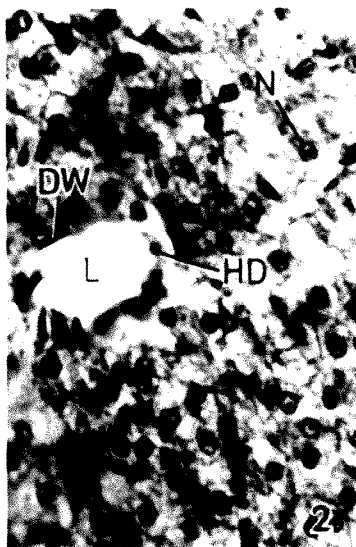
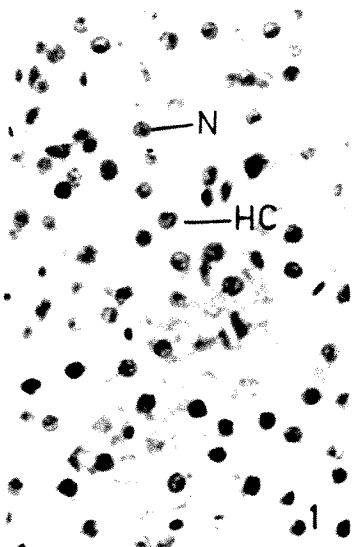
Very little alterations in the histological architecture of the liver occur at this concentration. The first sign of the toxic effect on liver cells was precipitation of the cytoplasmic contents and deformation in the arrangement of hepatocytes.

CAPITONS TO FIGURES

Plate No.3 : Histopathological changes in the liver of  
T. mossambica stained with H-E.

- Fig.1 T.S. of normal liver showing polyhydral hepatocytes (HC) with prominent nucleus (N) and nucleolus. X 200.
- Fig.2 A magnified view of T.S. of liver showing hepatocytes (HC) with nucleus, Hepatic duct (HD) with duct wall (DW). X 450.  
*Lumen (L), Nucleus (N)*
- Fig.3 T.S. of liver exposed to 1% conc. showing degenerating hepatocytes (HC), picnotic nuclei (N) and hepatic duct (HD) with debris in the lumen and thickened duct wall. X 400.  
*Duct wall (DW), Lumen (L)*
- Fig.4 T.S. of liver exposed to 1% conc. showing degenerating hepatocytes (HC) and swelling of nucleus (N). X 450.
- Fig.5 T.S. of liver exposed to 2% conc. and swollen nuclei (N). X 450. *Hepatocyte (HC)*
- Fig.6 T.S. of liver exposed to 2% conc. showing degenerated hepatocytes (HC), picnotic nuclei (PN) and swollen nuclei (N). X 450.
- Fig.7 T.S. of liver exposed to 3% conc. showing hepatic duct with luminal debris (L), degenerated duct wall (DW) and picnotic nuclei (PN). X 450. *Hepatic duct (HD)*
- Fig.8 T.S. of liver exposed to 3% conc. showing degenerated binucleated (BN) hepatocytes. X 450.
- Fig.9 T.S. of liver exposed to 4% conc. showing degenerated hepatocytes with swollen nuclei (N). Hepatic duct (HD) with luminal debris (LD). X 450. *Hepatocyte (HC)*
- Fig.10 T.S. of liver exposed to 4% conc. showing thickened hepatic duct wall (DW), lumen filled with debris (LD). X 200.  
*Lumen (L), Hepatocyte (HC)*
- Fig.11 T.S. of liver exposed to 5% conc. showing progressive degeneration of hepatic cells with swollen nuclei (N) and picnotic nuclei (PN). X 450. *Hepatocyte (HC)*
- Fig.12 T.S. of liver exposed to 5% conc. showing progressive degeneration of hepatocytes (HC), thickened hepatic duct wall (DW) and luminal debris (LD). X 450. *Nucleus (N)  
Hepatic duct (HD)*

# PLATE NO. 3



The nuclei of the hepatocytes showed swelling and picnosis (fig.3,4). Concentration of the nuclear material at the perinuclear region was another indication of nuclear changes. Nearly 30 to 40 % hepatocytes showed swelling and hypertrophy resulting into the displacement of nucleus. The central vein showed no alterations.

2% Conc. :

The precipitation of cytoplasmic content was more pronounced and formed reticular network in the hepatocytes. They were swollen to the maximum and showed large vacuoles (fig.5,6). Displacement of nuclei to the periphery of hepatocytes was observed. The cell boundaries were distinct (fig.5). Further enlargement of the nucleus occurred at this concentration. Some of the cells lost their nuclei (fig.5). Picnotic nuclei in a few hepatocytes were detected. Degenerative changes were also observed in the hepatocytes present at the peripheral part of liver.

3% Conc. :

Further enhancement in the pathological changes was evidenced at this concentration. The liver cells showed further enlargement and it led to the initiation of disorientation of the liver cord (fig.7,8). The hepatic cells with mitotic divisions were seen in the liver parenchyma (fig.8). The binucleated hepatocytes occurring at this concentration indicated the increase in mitotic activity. The degeneration of the nucleus was also observed. Such changes simultaneously showed gaps in the cordal arrangement, thus leading to the deformation in the histology of

the liver. Irregular shaped nuclei were very prominent at this stage. Hepatic ducts showed accumulation of debris in them.

4% Conc. :

The histopathological effects of distillery effluent were proportionately greater in the fishes exposed to 4% conc. The effects were significant in having the liver cord in disarray (fig.9). Hepatic cells with mitotic figures, binucleated hepatic cells with and without mitotic figures, swollen hepatocytes and atypical cells with greatly enlarged irregular shaped nuclei could also be seen (fig.9,10). Degeneration in hepatocytes led to the cluster formation of nuclei. Such clusters could be found throughout the tissue (fig.9). The central vein in the hepatic lobules was dilated. In it an accumulation of coagulated blood was clearly observed. Some degenerative changes were evident in certain part of the central vein.

5% Conc. :

Changes produced at this conc. were severe and highly chronic. Swelling and vacuolization in hepatic tissue was at its maximum and it was difficult to mark the cell boundaries (fig.11). Degenerative changes resulted in marked damage of the peripheral areas of the liver lobules. Cytoplasm of the hepatocytes was stained densely. Vacuolization, picnosis and surface irregularities in the nuclei were maximum (fig.11). The mitotic figures were seen occasionally (fig.11). In extreme cases an extrusion of nucleus from the cell was noted. These changes in hepatocytes caused gaps in the hepatic substance and hence

deformity in the cordal arrangement of the hepatic cells (fig.11). Disruption of the sinusoids led to filling of blood in the gaps formed due to the disintegration of hepatocytes. The hepatic ducts with thickened wall at some places showed an accumulation of debris in them. Thus, the main features of the histopathological changes exposed to acute concentration are :

- (i) Total loss of histological architecture.
- (ii) The maximum degenerative alterations of hepatocytes leading to necrosis and formation of gaps in the hepatic tissue.
- (iii) Irregular shaped nuclei with few mitotic figures.
- (iv) Accumulation of cell debris in the hepatic duct.

#### Pancreas :

Observation of the serial sections of the liver mass in I. mossambica showed occasional appearance of pancreatic tissue. The histological changes due to different concentrations of distillery effluent as mentioned above did not show significant pathological changes in Pancreatic mass. Occasional destruction of hepatocytes surrounding the Islets of Langerhans was evident.

#### Rasbora daniconius :

The histological structure of the liver of R. daniconius and the histopathological alterations induced in it due to the distillery effluent of various concentrations are shown in Plate No. 4 (fig.1-12).

#### Histology :

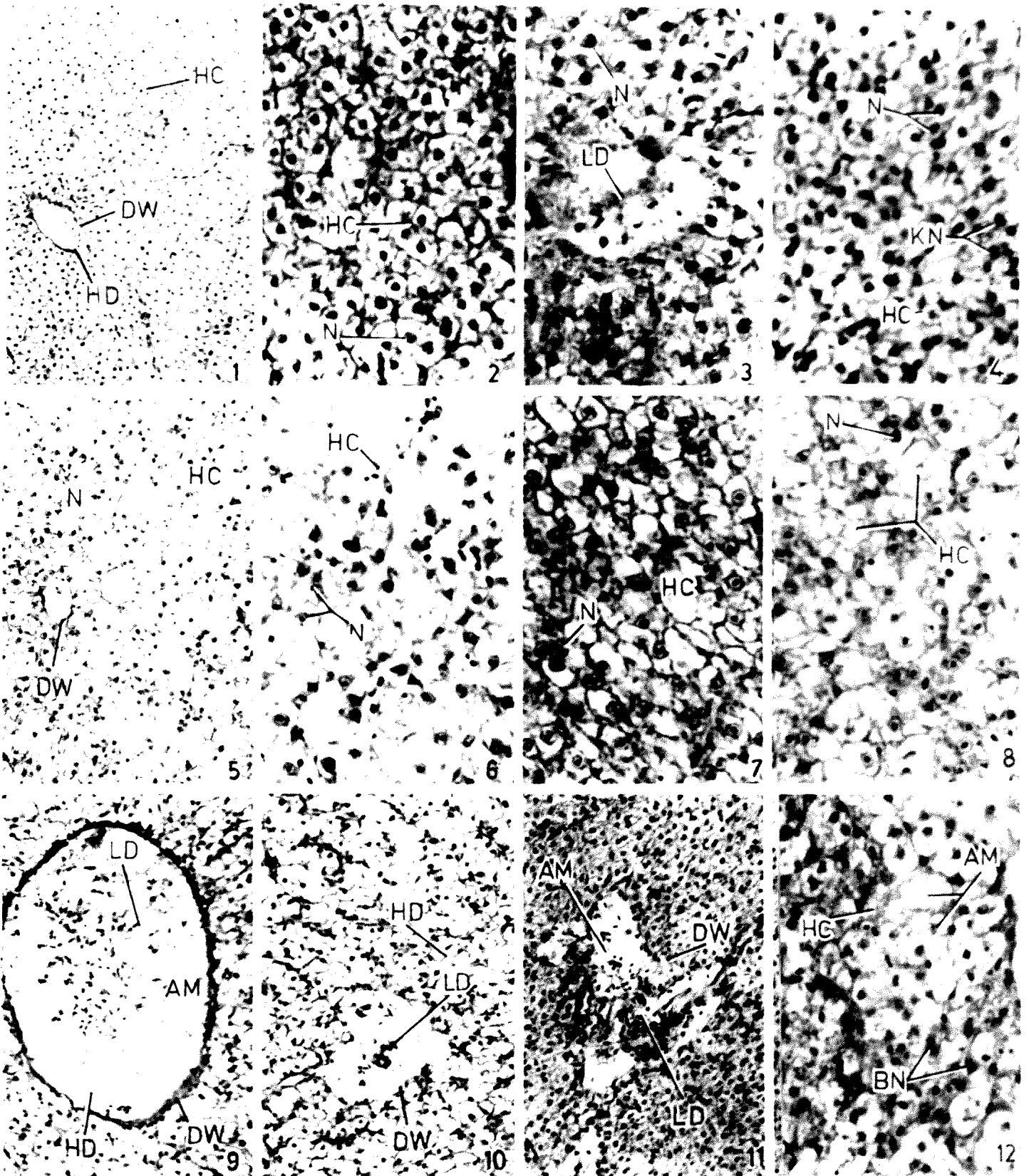
Histology of the normal liver of R. daniconius is

### CAPTIONS TO FIGURES

Plate No.4 : Histopathological changes in the liver of R.daniconius stained with H-E.

- Fig.1 T.S. of normal liver showing hepatocytes (HC) and hepatic duct (HD) and duct wall (DW). X 100.
- Fig.2 A magnified view of T.S. of liver showing polyhydral hepatocytes (HC) with prominent nucleus (N). X 450.
- Fig.3 T.S. of liver exposed to 1% conc. showing swelling of nucleus (N) and luminal debris (LD) in the hepatic duct. X 450.
- Fig.4 T.S. of liver exposed to 1% showing degenerating hepatocytes (HC), nuclear swelling (N) and karyolytic nuclei (KN). X 450.
- Fig.5 T.S. of liver exposed to 2% conc. showing degenerating hepatocytes (HC), Displacement of nucleus (N) and degeneration of duct wall (DW). X 200.
- Fig.6 T.S. of liver exposed to 2% conc. showing swelling of hepatocytes (HC) and extrusion of nuclei (N). X 450.
- Fig.7 T.S. of liver exposed to 3% conc. showing a distinct displacement of nuclei (N) and few hepatocytes (HC) devoid of nucleus. X 450.
- Fig.8 T.S. of liver exposed to 3% conc. showing degenerated hepatocytes (HC) devoid of nucleus and in few swelling of nucleus (N). X 450.
- Fig.9 T.S. of liver exposed to 4% conc. showing a prominent, thickened duct wall (DW) and luminal debris (LD) with some amorphous material (AM), X 200. *Hepatic duct (HD)*
- Fig.10 T.S. of liver exposed to 4% conc. showing degenerated hepatocytes with displaced nuclei, degenerated hepatic duct wall (DW) with luminal debris (LD). X 200. *Hepatic duct (HD)*
- Fig.11 T.S. of liver exposed to 5% conc. showing hepatic duct with luminal debris (LD) and amorphous material (AM), Nuclei are infiltrated due to the degeneration of duct wall (DW). X 200.
- Fig.12 T.S. of liver exposed to 5% conc. showing progressive degeneration of hepatocytes (HC) with vacuolization of hepatocytes showing amorphous material (AM) and few hepatocytes are binucleated (BN). X 450.

# PLATE NO. 4



practically identical to that of I. mossambica. The gall bladder of the former is smaller than the latter. The normal histological structure of liver of R. daniconius is shown in fig.1 and 2.

#### Histopathology :

The histopathological changes occurring in the case of liver of R. daniconius at different concentrations of the distillery effluent were nearly parallel to the histopathological changes of I. mossambica except in few histological details.

#### 1% Conc. :

At 1% concentration, there was an increase in the basophilic activity in the cell cytoplasm. Few cells contained granular cytoplasm on one side (fig.3). Most of the hepatocytes remained unaltered. In few hepatic cells the cytoplasmic accumulation displaced the nucleus towards the periphery (fig.3). In some cells the boundaries became diffused (fig.3). Their chromatin material showed an intense staining (fig.4). Some nuclei showed hypertrophy and formation of reticular chromatin material (fig.3). Hepatic duct wall was thick and its lumen contained bile secretion with pigment granules. Bile capillary, bile space and blood vessels remained unaltered (fig.3,4).

#### 2% Conc. :

At this exposure hepatocytes showed large number of degenerative changes. The first and most prominent change was swelling and vacuolization of the hepatocytes. It was accompanied by the loss of cytoplasmic contents and extrusion of nuclei (fig.6).

The extruded, hypertrophied picnotic nuclei formed groups and were scattered in the hepatic mass (fig.6). Some hepatocytes showed mitotic divisions. The accumulation of chromatin material at the centre and periphery was prominent. The hepatic duct wall became thin and degenerated at certain sites. In the hepatic sinuses black pigment granules were observed. Blood sinuses and blood vessels showed very few changes.

3% Conc. :

Histopathological changes increased progressively. These changes were characterised by the presence of extremely swollen liver cells. The liver cord was in complete disarray and there were also some surface irregularities. The disarray of the hepatic cord was because of the swelling of the hepatic cells (fig.8). The swelling was to such an extent that a large number of hepatocytes were destroyed and their nuclei became free and scattered in the hepatic mass (fig.8). Very few cells were with intact nucleus. The nuclei showed picnosis. Heterochromatin got accumulated at the periphery and the central part showed irregular nuclear surface. The cytoplasm of some hepatocytes were slightly stained. Mitotic figures were rarely seen. Prominent features of the pathological changes occurred at this concentration are : i) degeneration due to rupture and vacuolization of the hepatic cells, (ii) picnotic nuclei with irregular surface and (iii) cordal disarray.

4% Conc. :

The pathological alterations occurred at 3% and 4% were nearly identical. The edema of the hepatocytes became further

prominent and it led to the thinning of cell boundaries. The nuclei were displaced in few cases. Many were extruded out (fig. 10). The chromatin material also showed disintegration (fig.9). There was extreme dilation of hepatic duct. Its wall at certain places (fig.9), was diffused. Luminal contents were in the coagulated condition and showed ruptured blood cells with spindle shaped nuclei (fig.9). At the outer side of duct wall, there was peripheral accumulation of pigment granules (fig.9).

5% Conc. :

Pronounced toxicity showed a chronic effect on the liver tissue. The hepatocytes showed extreme vacuolization and edema (fig.12). Loss of nuclei from the hepatocytes and disintegration of hepatocytes produced intercellular spaces causing total cordal disarray and rupture of blood sinuses. The nuclei were irregular in their shape. Their structure was also deformed. Extruded nuclei were found to be accumulated at certain places (fig.12). The hepatic duct wall was totally disintegrated causing infiltration of extruded nuclei, blood cells and bile content in the tissues (fig.11). There was an increase in basophilic staining reactions of cytoplasmic granules. There was a loss of cell boundaries thereby difficult to make out the individual hepatocytes.

Pancreas :

AS in the case of I. mcssambica, R. daniconius showed few patches of Islets of Langerhans in the hepatic substance. The cells of the islets showed very little changes at lower concentra-

tion, However at the chronic exposure, islet cells showed slight hypertrophy and destruction of hepatic cells surrounding the islet thereby separating them from liver tissue.

(iii) KIDNEY :

Tilapia mossambica :

The normal histological structure and histopathological changes occurring due to the exposure of low and high concentrations of distillery effluent are shown in Plate No.5 (fig.1 to 12).

Histology :

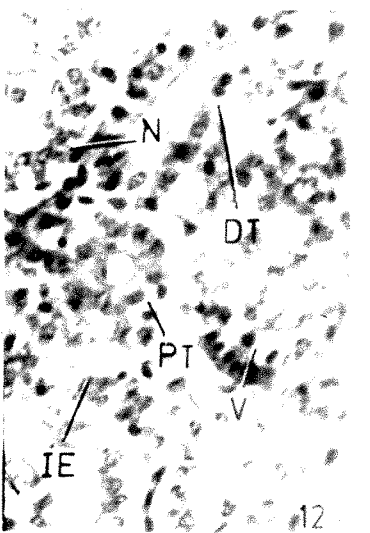
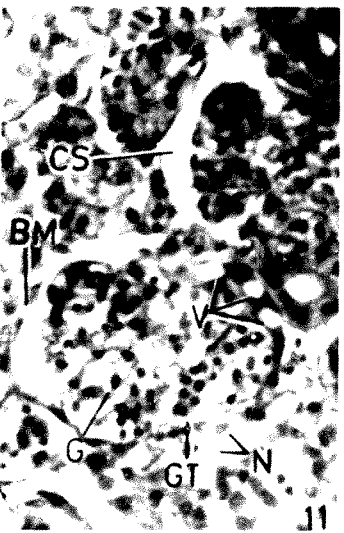
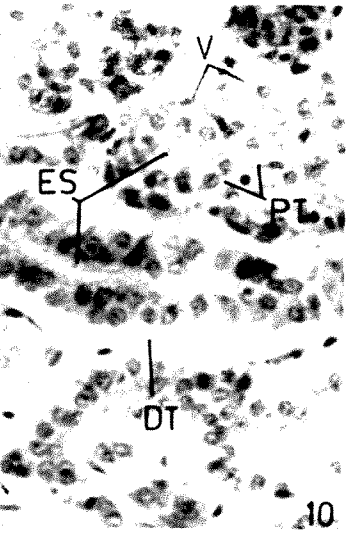
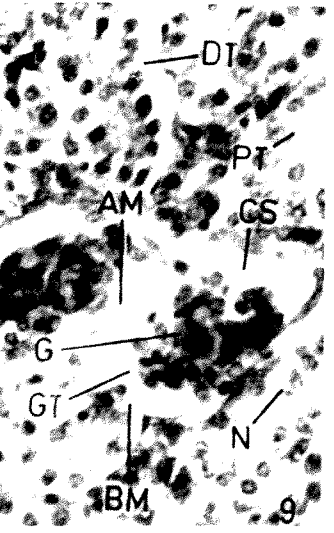
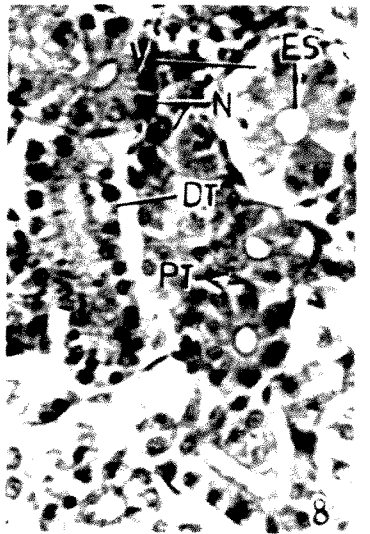
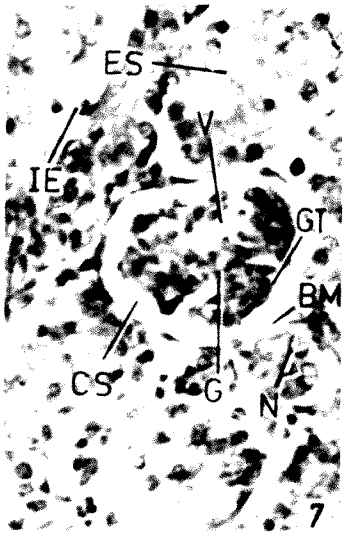
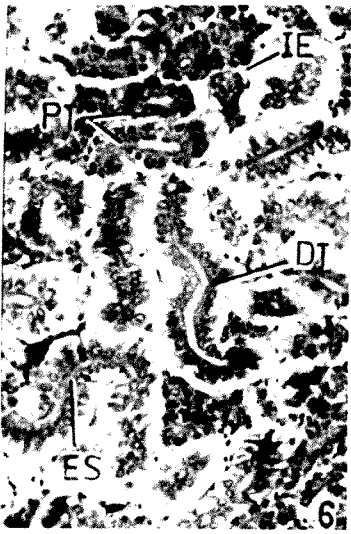
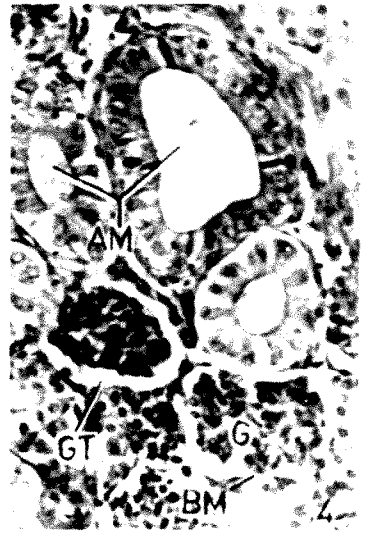
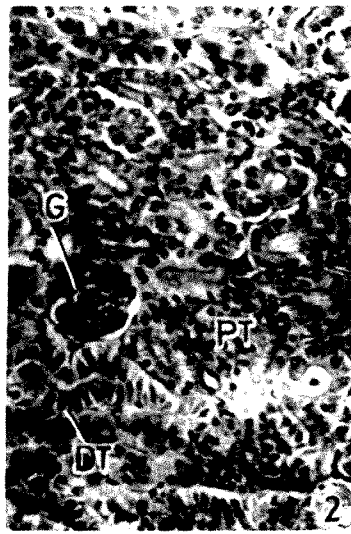
The histological structure of the kidney of T.mossambica resembled the structure in other fresh water teleosts. Anatomically it is differentiated into head kidney and trunk kidney. The head kidney contains more lymphoid and haemopoietic tissue and very little renal tissue. The structure of functional kidney (trunk kidney) consists of nephrons and Malpighian bodies (fig.1,2). Malpighian body constitutes Bowman's capsule enclosing a tuft of blood capillaries, the glomerulus. Bowman's capsule has basement membrane (fig.2). This is followed by a narrow neck, with ciliated epithelium which continues into proximal and distal tubules. Tall columnar epithelium of the proximal tubules show brush border towards the luminal side. The distal tubule ends into collecting duct. It has well developed epithelium. The interstitium of kidney substance shows groups of haemopoietic tissue.

## CAPTIONS TO FIGURES

Plate No.5 : Histopathological changes in the kidney of  
T. mossambica stained with H-E.

- Fig.1 T.S. of normal kidney showing glomerulus (G), proximal tubule (PT) and distal tubule (DT). X 100. Capsular space (CS) collecting tubule (CT)
- Fig.2 T.S. of kidney showing glomerulus (G), proximal tubule (PT) and distal tubule (DT). X 100.
- Fig.3 T.S. of kidney exposed to 1% conc. showing shrinkage of glomerulus (G), degeneration effected at proximal tubule (PT) and collecting duct (CT). X 200. Lumen (L)
- Fig.4 T.S. of kidney exposed to 1% conc. showing shrinkage of glomerulus (G), degeneration of basement membrane (BM), lumen of proximal tubule and collecting tubule showing amorphous material (AM). X 300. Glomerular Tuft (GT)
- Fig.5 T.S. of kidney exposed to 2% conc. showing shrinkage of glomerulus (G) and interstitial edema (IE) at some regions. X 200. Collecting tubule (CT)
- Fig.6 T.S. of kidney exposed to 2% conc. showing degeneration of proximal tubule (PT) and distal tubule (DT) swelling of nuclei interstitial edema (IE) and epith. swelling (ES) at some regions. X 200.
- Fig.7 T.S. of kidney exposed to 3% conc. showing degeneration of basement membrane (BM), glomerulus (G) showing vacuolization (V), Capsular space increased (CS), proximal tubule showing swollen nuclei, epithelial swelling (ES) at brush border and interstitial edema (IE) at few regions. X 450. Glomerular Tuft (GT)
- Fig.8 T.S. of kidney exposed to 3% conc. showing proximal tubules with nuclear swelling, epithelial swelling (ES) at brush border and vacuolization (V). Distal tubules showing nuclear swelling (N). X 450. Distal tubule (DT), Proximal Tubule (PT)
- Fig.9 T.S. of kidney exposed to 4% conc. showing progressive degeneration, basement membrane, obliteration, of glomerulus (G), increased capsular space (CS), filled with amorphous material (AM), progressive degeneration of proximal (PT) and distal tubule (DT). X 450. Nucleus (N), Basement membrane (BM), Glomerular Tuft (GT)
- Fig.10 T.S. of kidney exposed to 4% conc. showing progressive degeneration of epithelium of proximal tubule (PT) with vacuolization and epithelial swelling at brush border. Distal tubule (DT) showing nuclear enlargement and cellular degeneration X 450. vacuole (V), Epithelial swelling (ES).
- Fig.11 T.S. of kidney exposed to 5% conc. showing obliteration of glomerulus (G), with increased vacuolization (V) and increased capsular space (CS). Basement membrane showing progressive degeneration. X 450. Nucleus (N), Glomerular Tuft (GT), Basement membrane (BM)
- Fig.12 T.S. of kidney exposed to 5% conc. showing degeneration of epithelium of proximal tubule (PT) with nuclear enlargement and dist. tubule (DT) showing degeneration of epithelium with vacuolization. X 450. Vacuole (V), Nucleus (N),

PLATE NO. 5



Histopathology :1% Conc. :

No marked changes were detected in the kidney during earlier hours of the treatment. The histopathological changes were induced in fishes reaching asphyxiation.

The kidney appeared considerably swollen. The swelling was evidenced in the epithelia of proximal and distal tubules and glomeruli. Few cells of the collecting ducts were also enlarged. Vacuolization was apparent in the cytoplasmic contents of these cells. Hypertrophied nuclei showing irregular surface and vacuolization were seen (fig.3). The lumen of tubule was often reduced. Initiation of luminal dilation was prominent in collecting ducts. The brush border of proximal tubule showed disintegration. Disintegration of cytoplasmic material in a few proximal and distal tubule cells was noted (fig.4). Precipitation of cytoplasm and nuclear material in few renal tubule cells was also noted. Mild eosinophilic activity could be seen in cytoplasm of these cells. Karyolysis was another impact on these cells. Interstitial space remained unaltered. Renal corpuscle showed marked changes. The shrinkage of glomerular apparatus resulted in an increase in capsular size. The cells of haemopoietic tissue did not show any alterations. There was no evidence of the effect on blood supply and blood cells in the glomerular apparatus.

2% Conc. :

Pronounced changes leading to damage of the kidney tissue

were evidenced at this concentration. The damage was more in proximal and distal tubules. The precipitated substance in the renal cells got accumulated at the luminal side (fig.6). The swelling of the epithelia was further enhanced. It gave a honey-comb effect. The nuclei were displaced to the apical portion. Large number of nuclei showed karyolysis, vacuolization and disintegration of chromatin material (fig.6). Hypertrophy and edema of renal cells led to total disorientation of some renal tubules, thereby distorting the kidney structure. The glomeruli progressively showed shrinkage, thus creating more capsular space. Interstitium containing haemopoietic tissue showed hyperplasia, precipitation and picnotic nuclei. The damage in the capillaries was evidenced ~~the~~ by presence of blood cells in the intertubular space. The collecting ducts showed dilation of lumen, degeneration of basement membrane and nuclei of its cells (fig.6).

3% Conc. :

In addition to the above changes, pronounced and distinct pathological alterations took place at this concentration. The changes were characterised by destruction of proximal and distal tubules. Disintegration of nuclear material caused formation of vacuoles in nuclei (fig.7,8). Destruction of renal cells and loss of basement membrane of the tubules lead to the mixing of kidney tissue and formation of intertubular spaces (fig.7). The edema of the epithelial cells of collecting ducts and proximal tubule cells was highly pronounced (fig.8), thereby reducing the lumen of these ducts. Displacement of nuclei and picnosis was

evident. The haemopoitic tissue was severely affected. Destruction of endothelium caused diffused appearance in histological structure. Empty spaces at intervals in haemopoitic tissue indicated loss of some of the tissue material (fig.8).

4% Conc. :

Histological alterations were more or less identical as compared to above doses of distillery effluent. The prominent changes were honey combed effect, coalescence of adjacent renal tubules and interepithelial cells with picnotic nuclei (fig.9). Swelling of renal cells, shrinkage and degeneration of brush border was also observed. The glomerular apparatus was strikingly affected (fig.9). Disintegration of endothelial cells, creating empty spaces as well as shrinkage produced large capsular space. Karyolysis was evident cytoplasm showed intense eosinophilic activity. Intertubular space developed due to disintegration of renal cells and basement membrane. It showed presence of blood cells. Haemopoitic tissue was totally destroyed (fig.9,10).

5% Conc. :

The effects of lethal conc. of distillery effluent were severe. Excessive edema reduced the lumen of distal and proximal tubules. Their cytoplasm showed increased eosinophilic activity. The severe necrotic deformative changes in tubules were prominent (fig.12). Brush border of proximal tubule was totally lost. Nuclei were picnotic. Coagulation of chromatin material followed by fragmentation and loss of nuclei was evident (fig.11). The ultrafiltering apparatus of renal corpuscle was severely affected.

In few instances the extensive shrinkage caused accumulation of endothelial cells and it led to the formation of large capsular space. Other glomeruli showed damage of capillary network and loss of endothelial cells. Hence the appearance of glomerulus became diffused (fig.11). The cellular components of haemopoietic tissue appeared highly granular.

Rasbora daniconius :

Histology : (Plate No.6)

Histology of normal kidney of R. daniconius is similar to that of I. mossambica and other fresh water teleosts. It has usual head kidney with lymphoid and haemopoietic tissue (fig.1) and the trunk kidney composed of nephrons (fig.2).

Histopathology :

1% Conc. :

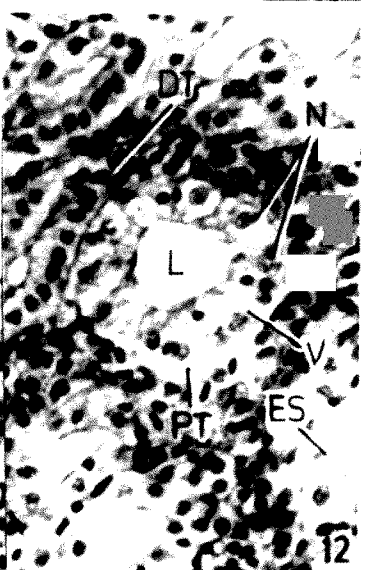
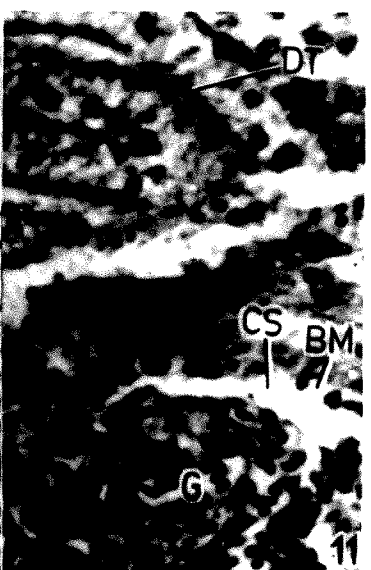
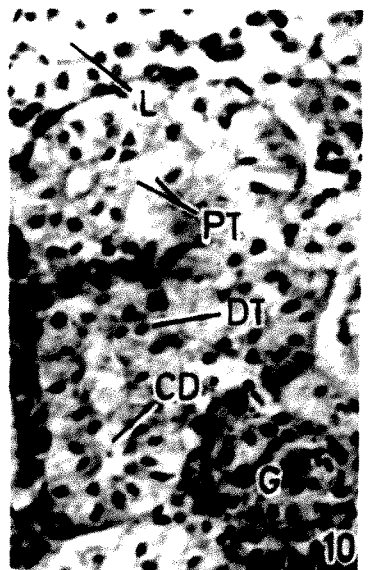
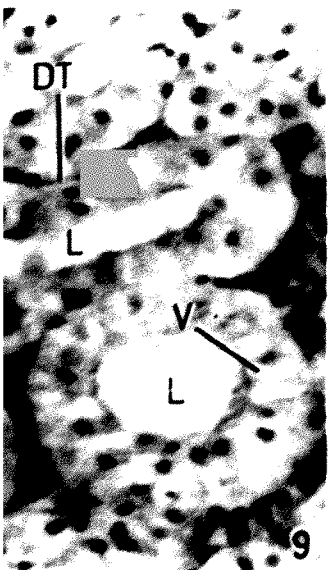
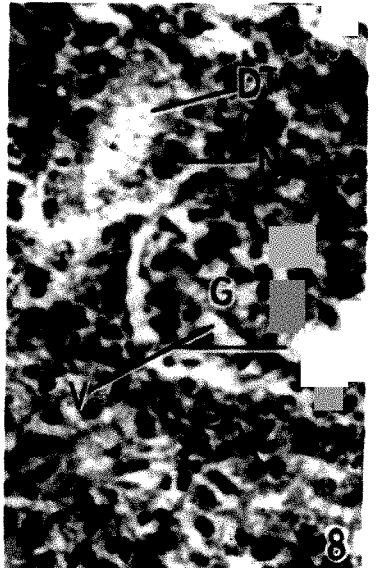
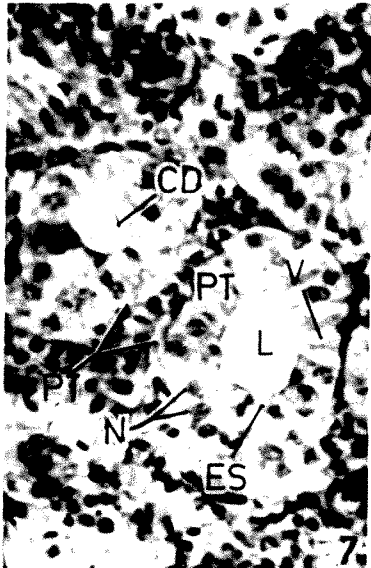
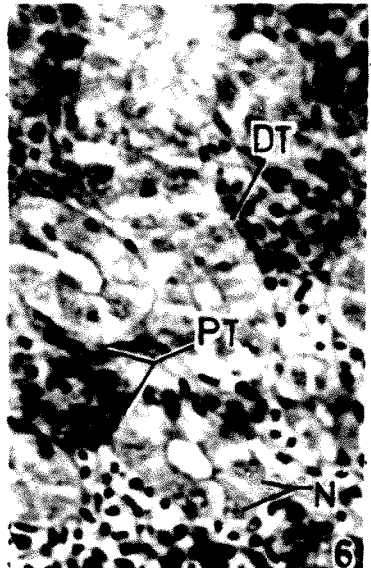
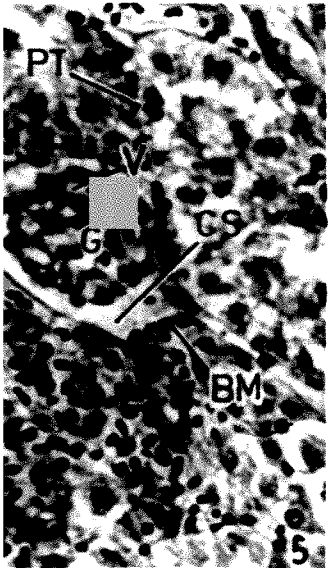
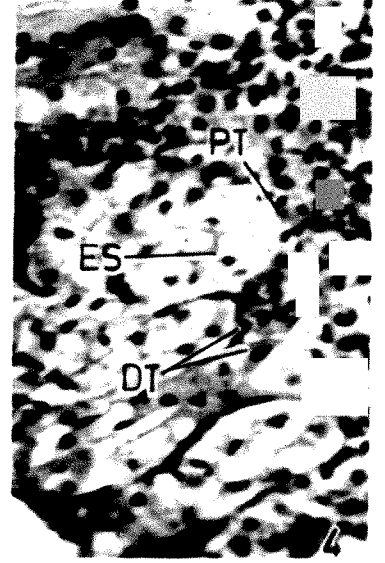
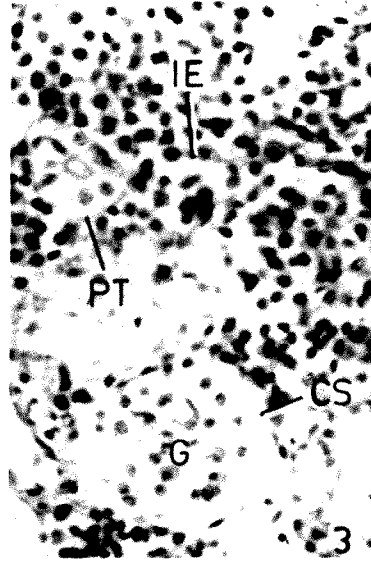
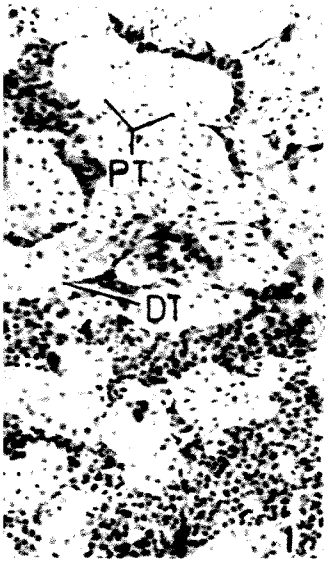
The alterations, occurring in the histological structure of the kidney are more or less parallel to those observed in the kidney of I. mossambica. The renal tubular cells were vacuolated and they were slightly swollen. They contained irregular and displaced nuclei (fig.3). The luminal portion of proximal and distal tubule was reduced, cytoplasm of renal cells showed slight eosinophilic activity. Very little changes occurred in the brush border of proximal tubules. The striking changes took place in the renal corpuscles. The hypertrophied endothelial cells with picnotic nuclei were found abundantly in the glomeruli (fig.3,4). Shrinkage was observed in few glomeruli, thereby creating,

## CAPTIONS TO FIGURES

Plate No.6 : Histopathological changes in the kidney  
of R.daniconius stained with H-E.

- Fig.1 T.S. of normal kidney showing proximal tubule (PT), distal tubule (DT). X 200.
- Fig.2 A magnified view of T.S. of normal kidney showing glomerulus (G) with Capsular space (CS) and basement number (BM). X 450.
- Fig.3 T.S. of kidney exposed to 1% conc. showing enlargement of glomerulus (G), swelling of proximal tubular epithelium (PT) and interstitial edema (IE) at some regions. X 450.  
Capsular space (CS),
- Fig.4 T.S. of kidney exposed to 1% conc. showing proximal tubule with epithelium swelling (ES) at brush border and nuclear displacement. Distal tubule showing cellular degeneration (DT). X 450. Proximal tubule (PT)
- Fig.5 T.S. of kidney exposed to 2% conc. enlargement of glomerulus (G), showing vacuoles (V), capsular space (CS) and degeneration of basement membrane (BM). X 450. Proximal tubule (PT)
- Fig.6 T.S. of kidney exposed to 2% conc. showing proximal tubule (PT) with enlarged and displaced nuclei (N), Degeneration of epithelium. X 450. Distal tubule (DT)
- Fig.7 T.S. of kidney exposed to 3% conc. showing proximal tubule with progressive degeneration of epithelium causing cellular infiltration and epithelial swelling (ES), Nuclei swollen and displaced, vacuolization (V). X 450. Proximal tubule (PT), Nucleus (N) Lumen (L), Collecting duct (CD)
- Fig.8 T.S. of kidney exposed to 3% conc. showing enlargement of glomerulus (G), with vacuolization (V), diminishing the capsular space, proximal tubule (PT) showing enlargement, displacement of nuclei and obliteration of cellular epithelium. X 450.  
Nucleus (N), Distal tubule (DT), Proximal tubule (PT)
- Fig.9 T.S. of kidney exposed to 4% conc. proximal tubule showing degeneration of cell epithelium, vacuoles (V). Few cells devoid of nucleus. Distal tubule (DT) showing progressive degeneration of cell epithelium. X 450.  
Lumen (L).
- Fig.10 T.S. of kidney exposed to 4% conc. proximal tubule (PT) showing increased degeneration, complete obliteration of cell epithelium. Distal tubule (DT) showing cellular degeneration with nuclear displacement. X 450. collecting duct, (CD), Lumen (L)
- Fig.11 T.S. of kidney exposed to 5% conc. Glomerulus (G) showing obliteration of basement membrane and vacuolization in capillary network. Distal tubule (DT) showing complete obliteration, with nuclear enlargement. X 450.  
Capsular space (CS), Basement membrane (BS)
- Fig.12 T.S. of kidney exposed to 5% conc. proximal tubule (PT), showing nuclear hypertrophy and progressive degeneration in cell epithelium with vacuolization (V). Distal tubules (DT) showing progressive cellular degeneration and epithelial swelling (ES). X 450. Nucleus (N)

PLATE NO. 6



a capsular space which was bound by basement membrane of the Bowman's capsule (fig.3). Very little changes were seen in haemopoitic tissue that lies in interstitium of the kidney.

2% Conc. :

The alterations occurring due to sublethal conc. of distillery effluent increased progressively.

Most evident changes took place in earlier segment of renal tubules. The epithelium of proximal tubules showed edema. Few cells showed degenerating fragmented nuclei (karyolysis) (fig.6). The histological observations at high power of microscope showed loss of integrity of kidney tubules (fig.6). The distal portion of proximal tubule also showed similar changes. The cytoplasm of uriniferous tubules showed increased eosinophilic activity. Loss of brush borders occurred in proximal tubules. The basement membrane that lines the tubule is totally lost. The collecting tubule cells showed displacement of nuclei from basal to apical portion. The glomeruli showed further shrinkage, thereby increasing capsular space containing fluid substance. The endothelial cells of glomeruli were intensely stained. The interstitium showed presence of blood cells. Haemopoitic tissue showed hypertrophy. Few picnotic nuclei stained intensely (fig.6).

3% Conc. :

Changes occurring at 3% conc. of distillery effluent on kidney were more or less identical to those occurring at 2% conc. The following alterations were acute and pronounced : i)



degeneration of epithelium of proximal and distal tubule.

(ii) Some picnotic nuclei were extruded. (iii) Brush border of proximal tubules was distorted. (iv) Collecting ducts showed enlarged lumen and hypertrophied epithelium. (v) Few cells showed karyolysis while others were with irregular nuclei. (vi) Glomeruli showed pronounced hypertrophy of endothelial cells, few disintegrated cells capsular space was more evident. (vii) The detached renal cells were scattered throughout the kidney substance. (viii) The haemopoitic tissue showed degeneration and loss of integrity. (ix) The eosinophilic activity in the cytoplasm of renal cells was intense.

#### 4% Conc. :

The renal damage became more severe and spread over to the entire kidney tissue. The protoplasmic material in proximal tubular cells had practically disappeared thereby showing less eosinophilic activity. The tubular structures of kidney were intermixed (fig.10). At certain places kidney tissue showed homogenous nature with scattered picnotic nuclei. It was because of loss of basement membrane. The renal corpuscles were more distorted (fig.10). The collecting ducts showed more or less similar changes as those observed at earlier concentrations. Haemopoitic tissue was severely affected, occasionally showing empty spaces indicating complete destruction of some of the tissue material. The blood capillaries showed desruption in glomerulus.

#### 5% Conc. :

The toxic effect of distillery effluent at 5% was very

severe and acute. The precipitation of protoplasm in most of the proximal tubule cells reached to its maximum. Hypertrophy of the epithelial lining of proximal and distal tubules was to such an extent that it led to the breaking of epithelial cells (fig.11). The damage of this tissue was all over the kidney, making it difficult to detect the kidney components (fig.11). Certain tubular portions were completely lost, thereby creating intercellular space, which was filled with fluid substance containing tissue debris. The glomeruli showed severe damage in endothelial cells and their nuclei (fig.11). Glomerular shrinkage was prominent, creating capsular space. The basement membrane of Bowman's capsule was lost totally.

The brush border of the proximal tubule was lost. The epithelium of collecting tubule showed swelling. Some of the epithelial cells of ducts showed loss of nuclei, thereby causing vacuolization. Few cells showed karyolytic activity and remaining were with prominent picnotic nuclei. Dilation in the duct lumen was evident and brush borders of the duct epithelium was less evident (fig.12).

Haemopoietic tissue cells were totally destroyed, with an exception of few blood <sup>cells</sup>, which were observed with cytoplasm and shrunken nuclei in the centre.

---